LATERAL FORCE CONTROL THROUGH ARMATURE CURRENTS IN SUPERCONDUCTING LSM MAGLEV VEHICLE

Tetsuzo Sakamoto.
Department of Control Engineering, Kyushu Institute of Technology
Tobata, Kitakyushu 804-8550, Japan

SUMMARY

The ride comfort or stability of the superconducting maglev vehicle is still the area to be investigated for commercial implementation. This paper proposes a method to get the vehicle guidance forces for a superconducting EDS maglev with LSM propulsion. The author has previously proposed a methodology of analysis using dq0 transformation with space harmonics included, and obtained the exact expression for the propulsion force in terms of q-axis component. It is shown that the d-axis components of the LSM armature currents result in lateral forces, and we show the formulation and design the vehicle motion regulator system, demonstrating the high performance by computer simulations.

INTRODUCTION

Superconducting magnetically levitated vehicle is suitable for super high-speed ground transport in terms of both electrical and dynamical characteristics. It includes three fundamental elements for producing propulsion, levitation and guidance forces with no contact. The vehicle of Japan Railway in Yamanashi is being tested for gathering data for a possible commercial operation in the near future. A traveling magnetic field generated by the linear synchronous motor (LSM) windings on the ground interacts with onboard superconducting magnets (SCMs), resulting in propulsion forces. The magnetic field of SCMs on the vehicle induces emfs in levitation-guidance coils on the ground, and the forces of levitation and guidance are produced.

One of the problems of the vehicle is that the ride comfort has not yet been gained as much as the designer expects. The spring constant in the lateral direction can be specified at the design stage, while the damping forces cannot be obtained satisfactorily. The actual damping relies on the uncertain phenomenon that could not be estimated. This causes a slight vibration with amplitudes of less than 10mm [1]. Moreover the minimum levitating speed should be preferably set as low as possible, but it is limited because even the spring constant is very weak at low speeds. These problems strongly motivate the study for additional guidance forces.

The author has previously proposed a methodology of formulation for the superconducting linear synchronous motor with the space harmonics of magnetic field included exactly, and then defined the thrust coefficient [2]. This formulation has now become the basis for studying the propulsion system quantitatively [3].

This paper presents the extension of our formulation to the lateral motion of the superconducting LSM, and a guidance force coefficient of the propulsion system is defined. The coefficients are calculated for the two types of feeding system: two-power converter system and three-power converter system. Then a method of generating desired lateral forces through propulsion coil currents is proposed, and the regulator system design methodology for the three-power converter system is proposed.

LATERAL FORCE AND ITS FORMULATION

It is convenient to consider the dq-frame when we discuss the electromagnetic forces for propulsion and guidance. Suppose the situation that the LSM armature coils, i.e. propulsion coils, and SCMs are positioned as shown in Figure 1(a). The symbols of dot and cross represent the positive directions for armature currents. If the armature currents have the values such that $i_U > 0, i_V > 0, i_W < 0$, then the currents, which can be replaced with the equivalent magnets, interact with the magnetic fields of SCMs. The forces are decomposed into the propulsion force and lateral force as shown in the figures (b) and (c), respectively. The arrow directing to the SCM indicates repulsive force while the opposite arrow means the attractive force. In this case, the phases V and W generate propulsion force, whereas the phase U generates the lateral force. On the dq-frame in which the d-axis is assigned to the field axis of SCMs, the former corresponds with the q-axis, and the latter with the d-axis. Therefore, it is found from these discussions that the q-axis and d-axis currents produce propulsion and lateral forces, respectively.

The magnetic coenergy stored between the armature and the SCMs is

$$W_m' = \begin{pmatrix} i_U \\ i_V \\ i_W \end{pmatrix}^T \begin{pmatrix} \psi_U \\ \psi_V \\ \psi_W \end{pmatrix} \quad \text{(J)} \tag{1}$$

where ψ_ς $(\varsigma = U,V,W)$ is the flux linkage of the armature windings, which is the function of the relative displacements of SCMs to the armature windings. Now we define the map of physical variables from the 3-phase axis to the $dq0$-axis

$$C = \sqrt{\frac{2}{3}} \begin{pmatrix} c_1 & c_2 & c_3 \\ -s_1 & -s_2 & -s_3 \\ \frac{1}{\sqrt{2}} & \frac{1}{\sqrt{2}} & \frac{1}{\sqrt{2}} \end{pmatrix} \tag{2}$$

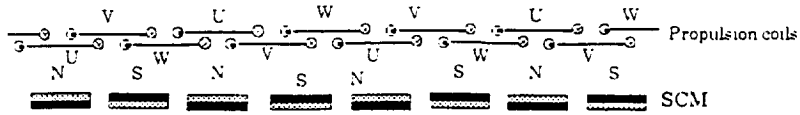

(a) Propulsion coils and SCMs

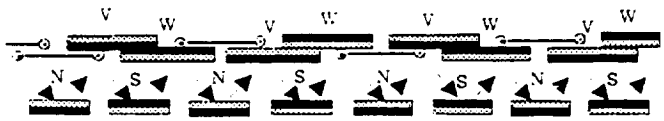

(b) Propulsion force component by the phases V and W

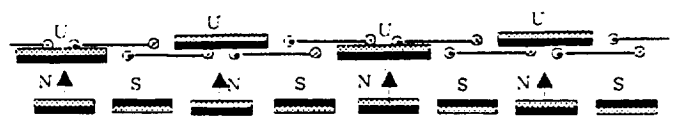

(c) Lateral force component by the phase U

Figure 1. Principles of forces by propulsion coil currents ($i_U > 0, i_V > 0, i_W < 0$)

where

$$c_1 = \cos\theta_{dq}, c_2 = \cos(\theta_{dq} - \frac{2\pi}{3}), c_3 = \cos(\theta_{dq} + \frac{2\pi}{3}) \quad , s_1 = \sin\theta_{dq}, s_2 = \sin(\theta_{dq} - \frac{2\pi}{3}), s_3 = \sin(\theta_{dq} + \frac{2\pi}{3}), \quad \theta_{dq} = \frac{\pi x_1}{\tau}$$

Substituting this into (1), we have

$$W_m' = \begin{pmatrix} i_d \\ i_q \\ i_0 \end{pmatrix}^T \begin{pmatrix} \psi_d \\ \psi_q \\ \psi_0 \end{pmatrix} \quad \text{(J)} \tag{3}$$

where

$$\begin{pmatrix} i_d \\ i_q \\ i_0 \end{pmatrix} = C \begin{pmatrix} i_U \\ i_V \\ i_W \end{pmatrix}, \quad \begin{pmatrix} \psi_d \\ \psi_q \\ \psi_0 \end{pmatrix} = C \begin{pmatrix} \psi_U \\ \psi_V \\ \psi_W \end{pmatrix}, \quad x_1 = v_x t \,, \quad v_x : \text{Vehicle speed}$$

Since we have obtained the energy in terms of currents and displacements, the lateral forces can be written by using the lateral displacement of the vehicle y_1 ($y' - y$; y', y : lateral axes fixed to the guideway and the vehicle, respectively) as follows

$$F_{Gpu} = \frac{\partial W_m'(i_d, i_q, i_0, y_1)}{\partial y_1} = i_d \frac{d\psi_d}{dy_1} + i_q \frac{d\psi_q}{dy_1} + i_0 \frac{d\psi_0}{dy_1} \quad \text{(N)} \tag{4}$$

Now we take up two models: one is a short vehicle equipped with the two-power converter system shown in Figure 2(a) and Figure 3(a), and the other is a long vehicle with the three-power converter system shown in Figure 2(b) and Figure 3(b). The flux linkages of the armature windings for one feeding section are given in the following equations:

$$\psi_U = \sum_{k=1,3,\cdots}^{\infty} \sum_{m=1,3,\cdots}^{\infty} \Psi_{km} e^{\beta_{km} y_1} \left[k_{ni} e^{\beta_{km} c_a/2} \sin\left\{ \alpha_k (x_1 + \frac{3\tau}{2}) \right\} + k_{no} e^{-\beta_{km} c_a/2} \sin\left\{ \alpha_k (x_1 - \frac{\tau}{2}) \right\} \right] \quad \text{(Wb)} \tag{5}$$

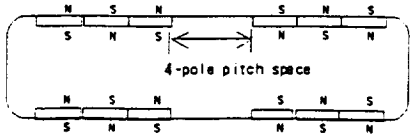

(a) A short length vehicle with doublefeeding system (model-1)

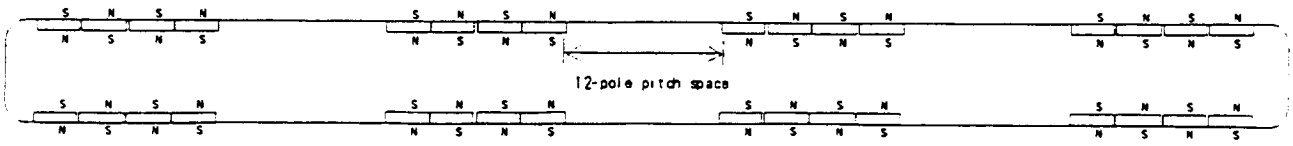

(b) A long length vehicle withtriple feeding system (model-2)

Figure 2. Schematic diagram of the vehicle models

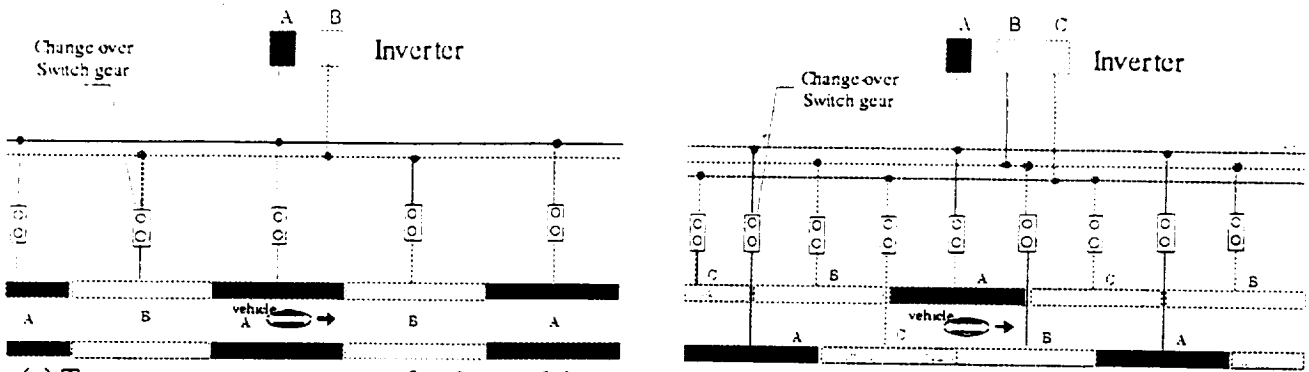

(a) Two-power converter system for the model-1 (b) Three-power converter system for the model-2

Figure 3. Feeding system

$$\psi_V = \sum_{k=1,3,\cdots}^{\infty}\sum_{m=1,3,\cdots}^{\infty}\Psi_{km}e^{\beta_{km}y_1}\left[k_{ni}e^{\beta_{km}c_a/2}\sin\left\{\alpha_k(x_1-\frac{7\tau}{6})\right\}+k_{no}e^{-\beta_{km}c_a/2}\sin\left\{\alpha_k(x_1+\frac{5\tau}{6})\right\}\right] \text{ (Wb)} \quad (6)$$

$$\psi_W = \sum_{k=1,3,\cdots}^{\infty}\sum_{m=1,3,\cdots}^{\infty}\Psi_{km}e^{\beta_{km}y_1}\left[k_{ni}e^{\beta_{km}c_a/2}\sin\left\{\alpha_k(x_1+\frac{\tau}{6})\right\}+k_{no}e^{-\beta_{km}c_a/2}\sin\left\{\alpha_k(x_1-\frac{11\tau}{6})\right\}\right] \text{ (Wb)} \quad (7)$$

where

$$\Psi_{km} = 2n_a\mu_0\frac{\beta_{km}}{\alpha_k\alpha_m}\sin(\alpha_k\frac{l_a}{2})\sin(\alpha_m\frac{w_a}{2})a_s(k,m)e^{-\beta_{km}(d_a-d_s)}\frac{\sin(N_a\alpha_k\tau)}{\sin(2\alpha_k\tau)}\cos\alpha_m z_1$$

$$a_S(k,m)=\begin{cases}\dfrac{32n_sI_s}{\pi^2km}\sin(\alpha_k\dfrac{l_s}{2})\sin(\alpha_m\dfrac{w_s}{2})\dfrac{\cos(3\alpha_k\tau/2)}{\cos(\alpha_k\tau/2)}\sin(5\alpha_k\tau/2) & \text{(model-1)}\\ \dfrac{64n_sI_s}{\pi^2km}\sin(\alpha_k\dfrac{l_s}{2})\sin(\alpha_m\dfrac{w_s}{2})\dfrac{\sin(2\alpha_k\tau)}{\cos(\alpha_k\tau/2)}\cos(16\alpha_k\tau)\cos(8\alpha_k\tau) & \text{(model-2)}\end{cases}$$

$\beta_{km}=\sqrt{\alpha_k^2+\alpha_m^2}$ $k_{ni}=n_{ai}/n_a, k_{no}=n_{ao}/n_a$, $\alpha_k=\pi k/L, \alpha_m=\pi m/W$, N_a : number of cells in one feeding section

n_sI_s : *mmf* of SCM, l_s, w_s : length and width of SCM, τ : pole pitch

n_{ai}, n_{ao}, n_a : number of turn of inner armature coil, outer coil, and and the average turn

n_a, c_a, l_a, w_a, d_a : number of turns, layer depth, coil length, coil width, position of armature windings

z_1 : center height difference between the armature and the SCMs

Combining (4) with (5), (6) and (7), we obtain the lateral force for the unit feeding section

$$F_{Gpu} = \sqrt{\frac{2}{3}}\sum_{k=1}^{\infty}\sum_{m=1}^{\infty}\beta_{km}\Psi_{km}e^{\beta_{km}y_1}\left\{k_d(x_1)i_d+k_q(x_1)i_q+k_0(x_1)i_0\right\} \quad \text{(N)} \quad (8)$$

where

$$k_d(x_1)=k_{ni}e^{\beta_{km}c_a/2}(c_1s_{u1}+c_2s_{v1}+c_3s_{w1})+k_{no}e^{-\beta_{km}c_a/2}(c_1s_{u2}+c_2s_{v2}+c_3s_{w2})$$

$$k_q(x_1)=-k_{ni}e^{\beta_{km}c_a/2}(s_1s_{u1}+s_2s_{v1}+s_3s_{w1})-k_{no}e^{-\beta_{km}c_a/2}(s_1s_{u2}+s_2s_{v2}+s_3s_{w2})$$

$$k_0(x_1)=k_{ni}e^{\beta_{km}c_a/2}(s_{u1}+s_{v1}+s_{w1})/\sqrt{2}+k_{no}e^{-\beta_{km}c_a/2}(s_{u2}+s_{v2}+s_{w2})/\sqrt{2}$$

$$s_{u1}=\sin\left\{\alpha_k(x_1+\frac{3\tau}{2})\right\}, \quad s_{u2}=\sin\left\{\alpha_k(x_1-\frac{\tau}{2})\right\}, \quad s_{v1}=\sin\left\{\alpha_k(x_1-\frac{7\tau}{6})\right\}, \quad s_{v2}=\sin\left\{\alpha_k(x_1+\frac{5\tau}{6})\right\}, \quad s_{w1}=\sin\left\{\alpha_k(x_1+\frac{\tau}{6})\right\},$$

$$s_{w2} = \sin\left\{\alpha_k(x_1 - \frac{11\tau}{6})\right\}$$

The lateral force consists of the three components: d-axis, q-axis, and 0-sequence forces. It is going to be demonstrated in the next **section** that the d-axis component is dominant and the other two components are very small compared to it. Accordingly, we can rewrite the equation as follows

$$F_{Gpu} = K_{Gp}(y_1,t)i_d + K_{Gpq}(y_1,t)i_q + K_{Gp0}(y_1,t)i_0 \quad \text{(N)} \tag{9}$$

where

$$K_{Gp}(y_1,t) = \sqrt{\frac{2}{3}} \sum_{k=1,3,\cdots}^{\infty} \sum_{m=1,3,\cdots}^{\infty} \beta_{km} \Psi_{km} e^{\beta_{km} y_1} k_d(x_1) \tag{10.a}$$

$$K_{Gpq}(y_1,t) = \sqrt{\frac{2}{3}} \sum_{k=1,3,\cdots}^{\infty} \sum_{m=1,3,\cdots}^{\infty} \beta_{km} \Psi_{km} e^{\beta_{km} y_1} k_q(x_1) \tag{10.b}$$

$$K_{Gp0}(y_1,t) = \sqrt{\frac{2}{3}} \sum_{k=1,3,\cdots}^{\infty} \sum_{m=1,3,\cdots}^{\infty} \beta_{km} \Psi_{km} e^{\beta_{km} y_1} k_0(x_1) \tag{10.c}$$

Since the d-axis component K_{Gp} is used to control lateral motions of the vehicle, we now call it the guidance force coefficient of the propulsion system.

CALCULATED RESULTS OF THE GUIDANCE FORCE COEFFICIENT

Figure 4(a) shows the guidance force coefficient for one feeding section at the left side as a function of time for the model-1 when the vehicle runs at 500km/h without lateral displacement $(y_1 = 0)$. The transients arise because it is assumed to have only one single feeding section. The plot indicates that guidance force may contain some pulsated forces, although the amplitudes are not so significant. It is found out that the harmonics are made from the 5-th and 7-th space harmonic fields. However, the

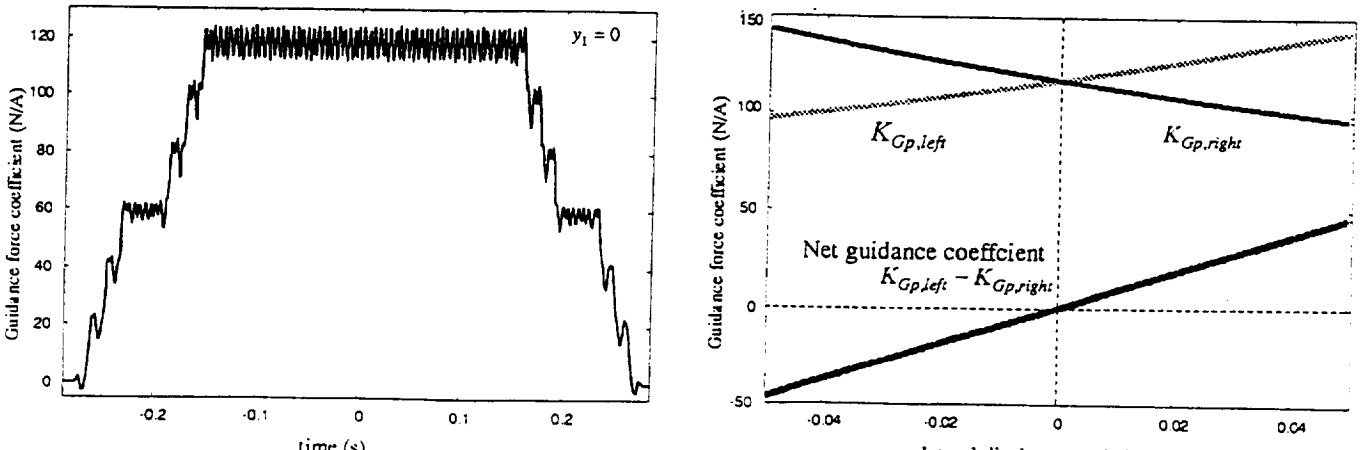

Figure 4. Guidance force coefficient (model-1; 500km/h)

model-1 has the two-power converter system, and accordingly the same armature current flows at both sides of feeding section. Therefore, the net guidance force coefficient is written as $K_{Gp,left} - K_{Gp,right}$, where the former is the one from the left side section, and the latter from the right section. This is shown in Figure 4(b). In this case, the vehicle guidance demands higher values of armature currents when the vehicle runs near the center of the guideway. To avoid this current capacity problem, the two sections at both sides of the vehicle should preferably be fed from different power supplies.

Figure 5 shows the calculated results for the model-2 with a three-power converter system, in which

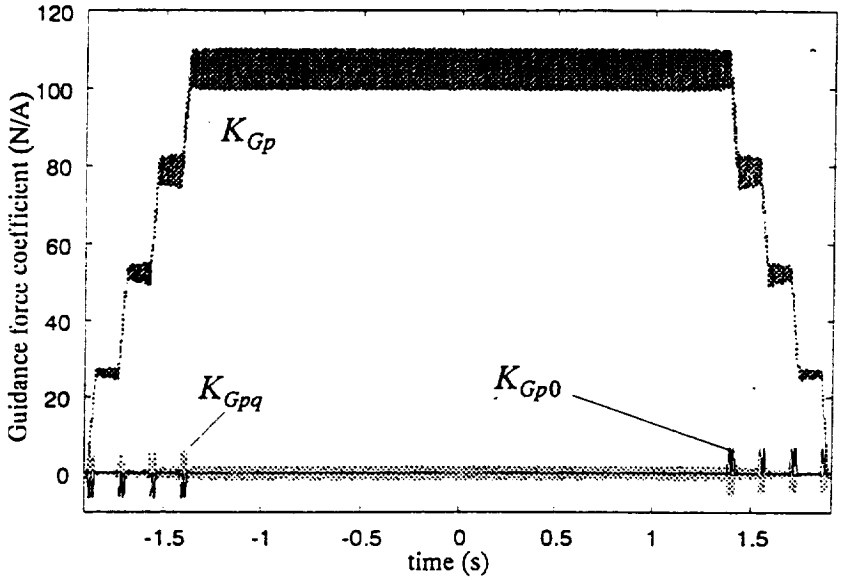

(a) Guidance force coefficient for unit section

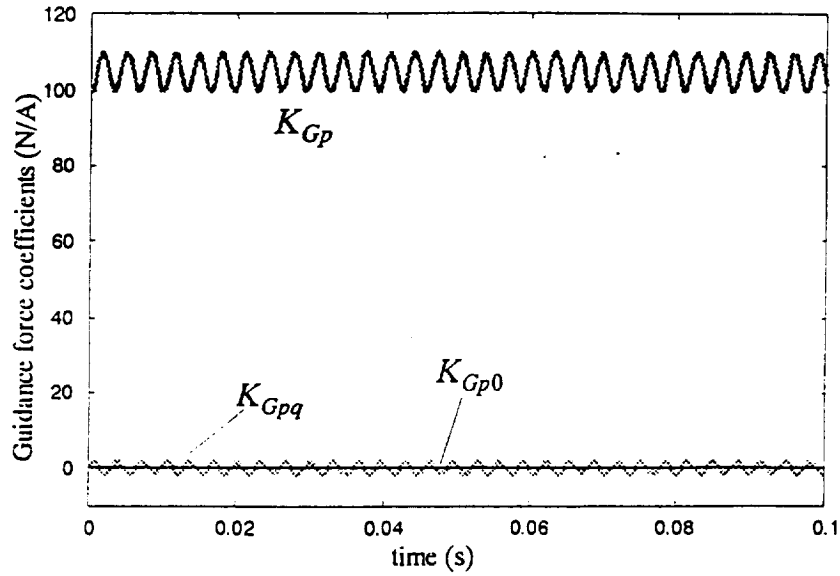

(b) Guidance force coefficents (close-up)

Figure 5. Guidance force coefficient
(model-2; 500km/h, z_1=0.04m)

every feeding section that faces the vehicle is supplied from a different source. The coefficients of (10) are plotted to compare the magnitudes. Positive value indicates that if the d-axis armature current is positive, the lateral force arises so that the lateral force y_1 increases, i.e., attractive force is generated between the armature and the SCMs. It is found that negative d-axis current should be supplied to the armature windings when the lateral displacement is positive: The q-axis has some ripples in the whole region, while the 0-sequence component is vanished except at the transient regions. Since the q-axis armature currents should be large enough to produce sufficient propulsion forces, rippled lateral forces may appear if only one side of q-axis current is especially enhanced. However, the same amplitude of q-axis armature currents is to be generated because propulsion force should be produced equally at both sides; there is no reason for enhancing one side of propulsion force. Therefore the both rippled forces cancel each other.

Figure 6 shows the coefficient as a function of lateral displacement. It is expected that the relation at the neighborhood of the center can be approximated by a linear function:

$$K_{Gp}(y_1,t) \cong K_{Gp0} + k_{Gp} y_1 \tag{11}$$

where

$$K_{Gp0} = K_{Gp}(0,t), \quad k_{Gp} = \left.\frac{\partial K_{Gp}(y_1,t)}{\partial y_1}\right|_{y_1=0}$$

LATERAL MOTION REGULATOR FOR VEHICLE

It was found out that the two-converter system might not fit into our guidance methodology using armature currents, and consequently our discussion for numerical simulations here for possible implementation is going to be focused on the model-2 with the three-converter system.

Our target is to build a regulator so that appropriate lateral guidance force is generated by armature

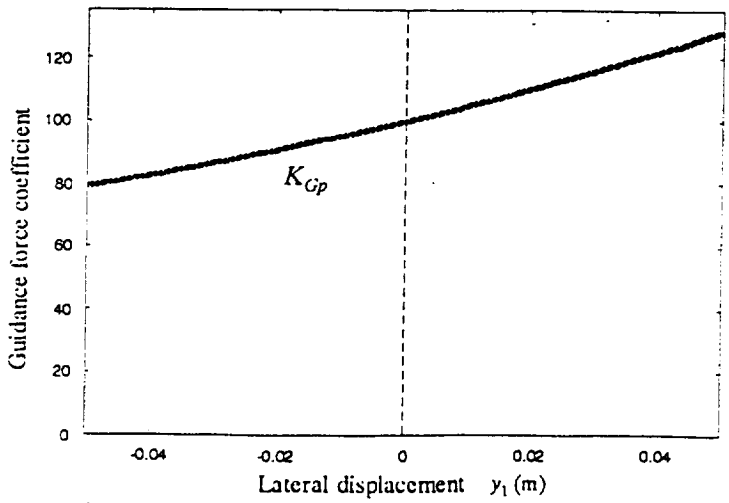

Figure 6. Guidance force coefficient of propulsion system as a function of lateral displacement

windings when the vehicle begins lateral motions triggered by some disturbances such as strong wind, guideway irregularities, etc. Figure 7 shows the concept of the regulator, where M is the vehicle mass, F is the feedback gain matrix, and K_{yy} is the spring constant of the levitation-guidance coils, which are installed along with the propulsion coils on the guideway. When the state vector comprised of lateral displacement and its time derivative has moved away from the equilibrium point, the state vector can be moved back by using a negative feedback of the vector to cancel the motions.

The regulator block diagram is shown in Figure 8, where the system has three controlled power sources corresponding to the three feeding sections. Instead of using the combination of the state feedback and feedback gain matrix, an output feedback is employed with a dynamic compensator $C(s)$: the negative feedback is given by

$$i_d = -Fx = -(f_1, f_2)(y_1, \frac{dy_1}{dt})^T = -f_1 y_1 - f_2 \frac{dy_1}{dt} \tag{12}$$

Using the Laplace transform, we have

$$I_d(s) = -(f_1 + f_2 s)Y_1(s) = -K_c(1 + T_{cd}s)Y_1(s) = -C(s)Y_1(s) \tag{13}$$

where $C(s) = K_c(1 + T_{cd}s)$.

If a feeding section is located on the left side of the vehicle, positive d-axis currents produce attractive

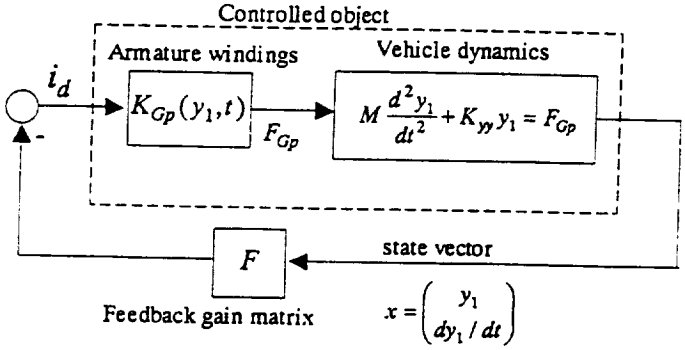

Figure 7. Concept of lateral motion regulator

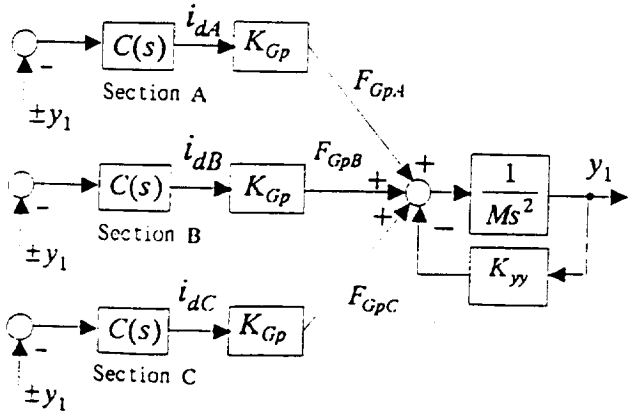

Figure 8 Vehicle lateral motion regulator system

force, i.e., positive force so that lateral displacement increases. When the feeding section is on the right side, it becomes a negative force. Therefore the guidance force coefficient K_{Gp} has different sign and function depending on which side of the vehicle the feeding section is located. Moreover a positive value of lateral displacement means that the vehicle is coming closer for the left side section, but moving away for the right side section. Then the control actions to cancel the vehicle motion should be the opposite from each other. The signs of y_1 in the figure indicate this situation.

The block diagram of Figure 8 is simplified to the diagram of Figure 9, being used for designing the dynamic compensator. Since the two sections at both sides of the vehicle are expected to generate the guidance force at the same time, one of them produces half the necessary force. Then the dynamic equation of the regulator observed from one section is written as

$$\frac{d^2y_1}{dt^2} + \frac{1}{M'}K_{Gp0}K_cT_{cd}\frac{dy_1}{dt} + \frac{1}{M'}(K'_{yy} + K_{Gp0}K_c)y_1 = 0 \tag{14}$$

where $M' = M/2, \quad K'_{yy} = K_{yy}/2$

This equation has the form of the standard second-order system

$$\frac{d^2y_1}{dt^2} + 2\zeta\omega_n\frac{dy_1}{dt} + \omega_n{}^2y_1 = 0 \tag{15}$$

As the result, our specification work for the regulator design has just become determining the damping factor and natural frequency. This is practically useful because we know the characteristics well. The spring constant of the levitation-guidance coils K_{yy} varies as the vehicle running speed changes. Accordingly, the proportional gain of the compensator K_c is to be altered based on a scheduling data if the natural frequency should be kept constant.

Assuming that $K_{yy} \cong 0$ at very low speed, the proportional gain is obtained by specifying the natural frequency ω_n as follows

$$K_c = \frac{M'\omega_n{}^2}{K_{Gp0}} \tag{16}$$

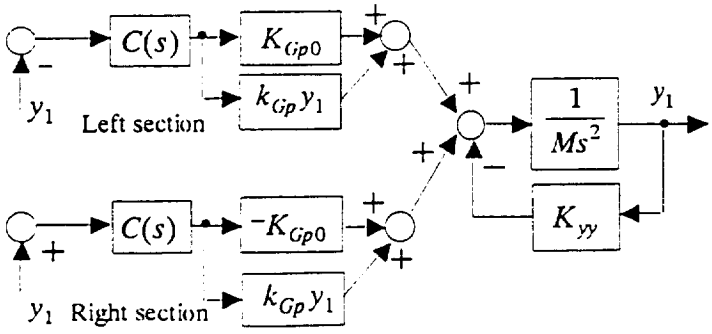

Figure 9. Simplified block diagram of the regulator

The derivative time is then determined by specifying the damping factor ζ, i.e.

$$T_{cd} = \frac{2\zeta\omega_n M'}{K_{Gp0}K_c} \tag{17}$$

To avoid a noise problem for sensing the lateral displacement, the addition of a low pass filter to the derivative term may be useful. If we consider the derivation frequency range to be less than ω_{der} (rad/s), then the dynamic compensator is finally constructed as

$$C(s) = K_c\left(1+\frac{T_{cd}s}{1+s/\omega_{der}}\right) \tag{18}$$

Figure 10 shows the simulations for the proposed regulator system using the block diagram of Figure 9. The assumed natural frequency is 10 (rad/s) with the damping factor of 0.5, 1 and 2. The vehicle was assumed to have a lateral disturbance force of 10,000 (N) as shown in the figure, which is equivalent to 20 (m/s) of lateral wind. From the results, the regulator works very well to suppress the vehicle motion in less than about 1(mm). Since the currents of the two sections have almost the same amplitude with an opposite sign, only the currents of the left side are depicted here. The currents are required only around 100(A) at most. The desirable damping factor may be 1 as expected.

CONCLUSIONS

The paper has presented the formulation of lateral forces resulting from the interactions between the armature coil currents and the SCMs, and proposed the vehicle guidance system by using the *d*-axis currents. The guidance force coefficient of the propulsion system was then defined. And the lateral motion regulator system was proposed together with the design methodology, where the design formula has become the problem of determining the damping factor and natural frequency of lateral vehicle motion. Finally the numerical demonstration has shown that the system works very well.

REFERENCES

1. H.Yoshioka et al., Results of Running Tests and Characteristics of the Dynamics of the MLX01 Yamanashi Maglev Test Line Vehicles, Proc.MAGLEV'98, pp.225-230
2. T.Sakamoto, Analysis of a Superconducting Linear Synchronous Motor Propulsion in terms of *dq* variables, *Trans. IEE of Japan*, vol.116-D, No.2, pp.177-182, 1996
3. T.Sakamoto, Investigation of Superconducting Linear Synchronous Motor Propulsion Control via an Exact Mathematical Model, *Trans. IEE of Japan*, Vol.118-D, No.5, pp.572-578 (1998)

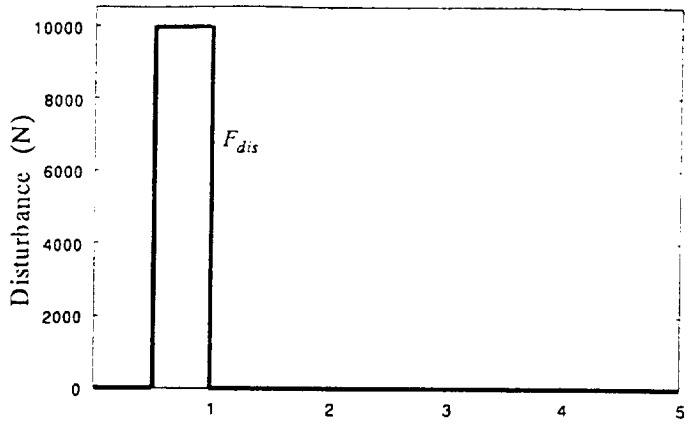

(a) Disturbance force

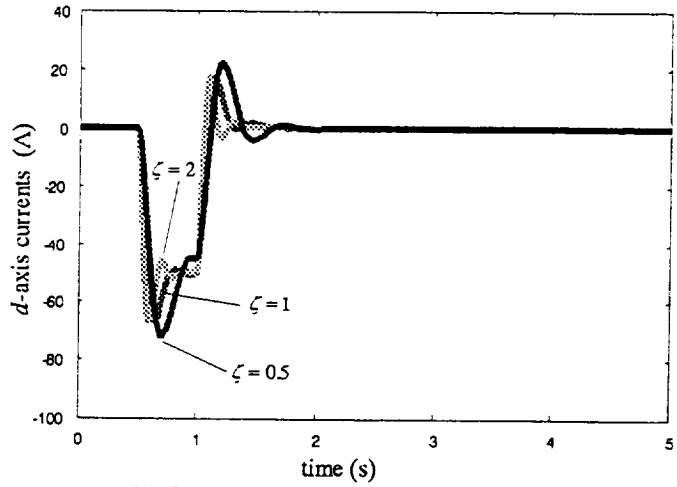

(b) d-axis currents (left side of the vehicle)

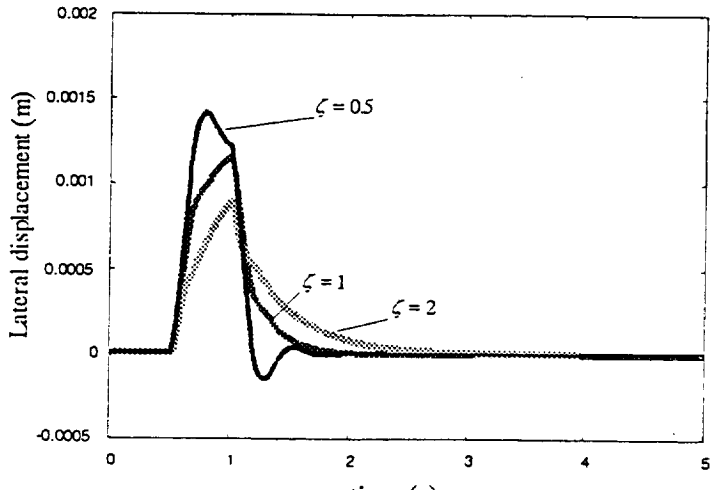

(c) Lateral displacement

Figure 10. Regulator simulation